

Isolated pulsar spin evolution on the $P-\dot{P}$ Diagram

J.P. Ridley¹ and D.R. Lorimer^{1,2}

¹*Department of Physics, West Virginia University, PO Box 6315, Morgantown, WV 26506, USA*

²*National Radio Astronomy Observatory, PO Box 2, Green Bank, WV 24944, USA*

Accepted 2010 January 13. Received 2009 December 21; in original form 2009 July 15

ABSTRACT

We look at two contrasting spin-down models for isolated radio pulsars and, accounting for selection effects, synthesize observable populations. While our goal is to reproduce all of the observable characteristics, in this paper we pay particular attention to the form of the spin period vs. period derivative ($P-\dot{P}$) diagram and its dependence on various pulsar properties. We analyse the initial spin period, the braking index, the magnetic field, various beaming models, as well as the pulsar’s luminosity. In addition to considering the standard magnetic dipole model for pulsar spin-down, we also consider the recent hybrid model proposed by Contopoulos & Spitkovsky. The magnetic dipole model, however, does a better job of reproducing the observed pulsar population. We conclude that random alignment angles and period dependent luminosity distributions are essential to reproduce the observed $P-\dot{P}$ diagram. We also consider the time decay of alignment angles, and attempt to reconcile various models currently being studied. We conclude that, in order to account for recent evidence for the alignment found by Weltevrede & Johnston, the braking torque on a neutron star should not depend strongly on the inclination. Our simulation code is publically available and includes a web-based interface to examine the results and make predictions for yields of current and future surveys.

Key words: pulsars: general – pulsars: simulations

1 INTRODUCTION

The statistical properties of the radio pulsar population provide valuable constraints on the birth properties, evolution and radio lifetimes of neutron stars and have been the subject of many studies over the years (see, e.g., Gunn & Ostriker 1970; Taylor & Manchester 1977; Lyne et al. 1985; Narayan & Ostriker 1990; Bhattacharya et al. 1992; Johnston 1994; Lorimer et al. 1997; Hartman et al. 1997; Arzoumanian et al. 2002; Gonthier et al. 2002; Faucher-Giguère & Kaspi 2006). A key diagram to reproduce is the logarithmic plot of pulsar periods, P , and their rates of slowdown, \dot{P} , usually referred to as the $P-\dot{P}$ diagram. The many factors that affect the distribution of pulsars on the $P-\dot{P}$ diagram include the evolution of pulsars’ spin-down, luminosity, age, magnetic field, beaming, and the angle between the magnetic field and the rotation axis. While each parameter individually affects how pulsars evolve across the diagram, covariances between multiple parameters also influence the results.

The goal of this paper is to compare two pulsar spin-down models using Monte Carlo simulations of the Galactic young pulsar population. The first model we consider treats the pulsar as a rotating magnetic dipole from which there

is a simple relationship between the braking torque and the magnetic field (Gold 1968; Pacini 1968). This model has been used extensively in pulsar population studies in the past (see, e.g. Lyne et al. 1985; Narayan & Ostriker 1990; Bhattacharya et al. 1992) and has most recently been implemented by Faucher-Giguère & Kaspi (2006), hereafter FK06. In this paper, we desire to undergo a direct comparison of their results with our simulations.

The other model we consider, by Contopoulos & Spitkovsky (2006), hereafter CS06, treats the pulsar as a combination of a misaligned magnetic dipole rotating in vacuum and an aligned magnetic dipole rotating in an atmosphere with ideal magnetohydrodynamic conditions. In addition to implementing these two models with parameters as described in detail in FK06 and CS06, we investigate the effects of changing one or more of the assumptions made by these authors in an attempt to obtain a more accurate interpretation of the relationships between these parameters and the resulting $P-\dot{P}$ diagram.

As described in Section 2, we have created a computer simulation package which implements the above models and allows us to simulate the distribution of pulsars in the Galaxy and change the individual properties of each one. By

“observing” this population with accurate models of completed pulsar surveys (Section 3), we are able to create a simulated sample and compare its properties to those of the real observed sample. In Section 4 we briefly describe our method for comparing two population samples. In Section 5, we present and discuss our results. Our main conclusions are summarized in Section 6. To facilitate comparison with other studies, and provide a tool for the community, a major feature of this work is to make our simulation code freely available on a website which is discussed in Appendix A.

2 MODELING THE UNDERLYING PULSAR POPULATION

The computer program we have developed for this work, *evolve*, is an extension of the software package, *psrpop* which was initially developed to study the Galactic distribution of pulsars detected in the Parkes Multibeam surveys (Lorimer et al. 2006). For that work, time-independent pulsar populations were synthesized and compared to the observed sample. The main aim of this paper is to develop a time-dependent model of the population and is realized through a program we call *evolve*. In this section, we describe the logical flow of the program which determines first whether a model pulsar is potentially observable (i.e. is radio loud and beaming towards us), before computing any kinematic or spatial parameters.

The first step is to randomly assign an age, t , and a magnetic field, B , to each pulsar. The age is selected between 0 and t_{\max} , with t_{\max} being 10^9 years. As per FK06, the magnetic field is determined by a log-normal distribution, centred around a mean value, $\mu_{\log B} = 12.65$, with a standard deviation $\sigma_{\log B} = 0.55$. The initial period, P_0 , is then randomly generated. Following FK06, P_0 is chosen from a Gaussian distribution centred around $\mu_P = 300$ ms with a standard deviation $\sigma_P = 150$ ms.

We next compute the inclination angle between the magnetic field axis and spin axis, χ . In implementations of the magnetic dipole model, it is usually assumed (see, e.g., FK06) that $\chi = 90^\circ$. However, a more realistic model would account for a distribution of χ and use this information in a self-consistent way when calculating the beaming fraction discussed below. We explore a number of options, first fixing $\chi = 90^\circ$, and subsequently considering a random distribution of angles by selecting $\cos \chi$ from a flat distribution between 0 and 1. The latter choice effectively orients the magnetic axis as a uniform random vector over 4π sr. Finally, following recent empirical evidence in favour of a secular decay of χ with time (Weltevrede & Johnston 2008, hereafter WJ08), we also consider an exponentially decaying model defined as

$$\sin \chi = \sin \chi_0 \exp(-t/t_d), \quad (1)$$

where χ_0 is the initial angle (which we again choose by selecting $\cos \chi_0$ from a 0–1 flat distribution), and t_d is the $1/e$ decay timescale. Note that we choose this decay law over the one considered by WJ08 for mathematical and computational convenience. As shown in Fig. 1, the two dependencies give similar results. The braking index, n , is then assigned. In general, n is related to ν , the frequency of rotation, $\nu = 1/P$, and its time derivative

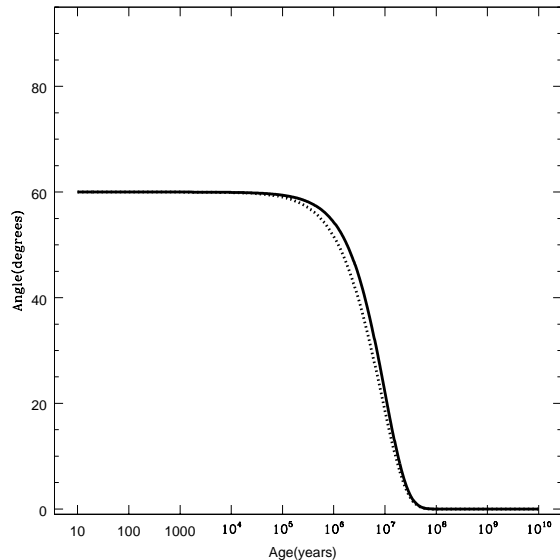


Figure 1. The time dependence of the alignment angle shown for Equation 1 (dotted curve) and the model used in WJ08 (solid curve). We use 60° for a reference as roughly half of all angles will be above and half will be below that value for a given random distribution of angles.

$$\dot{\nu} = -K\nu^n, \quad (2)$$

where K is a constant that depends on the pulsar’s moment of inertia and radius (see, e.g. Lorimer & Kramer 2005). We can use a single index for all pulsars, or randomly assign an index to each pulsar. Specific choices depend on the spin-down model under consideration which are described below.

Each spin-down model yields a time-dependent equation for the pulsar’s period and period derivative. The pulsar’s period evolves in time depending on the spin-down model, the magnetic field, the braking index, and the alignment angle. Considering first the magnetic dipole model, the period dependence can be found by solving

$$P^{n-2}\dot{P} = kB^2 \sin^2 \chi(t), \quad (3)$$

where $\sin \chi(t)$ is defined by Equation 1. The constant

$$k = \frac{8\pi^2 R^6}{3Ic^3}, \quad (4)$$

where R is the radius of the neutron star, assumed to be 10 km, and I is the moment of inertia, assumed to be 10^{38} kg m². For this choice of parameters, k takes the numerical value 9.768×10^{-40} , B is in units of Gauss while P , P_0 and t are in seconds.

The implementation of this model in FK06 assumes $n = 3$ and $\chi = 90^\circ$. In this case, the period dependence

$$P(t) = \sqrt{P_0^2 + 2kB^2t}. \quad (5)$$

More generally, for any braking index other than $n = 1$, and a constant value of χ , we find

$$P(t) = [P_0^{n-1} + (n-1)kB^2t \sin^2 \chi]^{\frac{1}{n-1}}. \quad (6)$$

Finally, extending this result for a time dependent inclination angle of the form assumed in Equation 1, we find

$$P(t) = \left[P_0^{n-1} + \frac{(n-1)}{2} t_d k B^2 \sin^2 \chi_0 (1 - e^{-2t/t_d}) \right]^{\frac{1}{n-1}}. \quad (7)$$

Depending on the model under consideration, one of Equations 5–7 is used to calculate the pulsar’s current period, P . Equation 3 is then used to find the corresponding value of \dot{P} . At this point, a simple test is made to determine if the pulsar has crossed the so-called death line. The death line signifies when a pulsar becomes radio-quiet, and Bhattacharya et al. (1992) quantified it as the locus of points for which

$$\frac{B}{P^2} = 0.17 \times 10^{12} \text{ G s}^{-2}. \quad (8)$$

If the pulsar has crossed the death line, the simulation marks the pulsar as dead (i.e. radio quiet) and moves on to create the next pulsar. If the pulsar has not crossed the line, then we continue on with the simulation. It should be noted, however, that a small number of pulsars (e.g. J2144–3933; Young et al. 1999) have crossed this theoretical line and are still observable at radio frequencies.

For our implementation of the CS06 model, the technique is slightly different. The time evolved period and period-derivative are calculated by integrating and then numerically solving

$$\dot{P} = 3.3 \times 10^{-16} \left(\frac{P}{P_0} \right)^{2-n} \left(\frac{B}{10^{12} \text{ G}} \right)^2 \left(\frac{P_0}{1 \text{ s}} \right)^{-1} \left(1 - \frac{P}{P_{\text{death}}} \cos^2 \chi \right), \quad (9)$$

where

$$P_{\text{death}} = \left[0.81 \times \left(\frac{B}{10^{12} \text{ G}} \right) \left(\frac{1 \text{ s}}{P_0} \right) \right]^{\frac{2}{n+1}} \text{ s}. \quad (10)$$

In this case, the pulsar is declared dead when the period becomes greater than P_{death} .

To account for the fact the pulsar radiation is only beamed to some fraction of 4π sr, a variety of beaming models have been implemented in *evolve*. The default model is from the work of Tauris & Manchester (1998), henceforth TM98, who found an empirical relationship for the fraction of the whole sky illuminated by a pulsar:

$$f(P) = 0.09 \left[\log \left(\frac{P}{1 \text{ s}} \right) - 1 \right]^2 + 0.03. \quad (11)$$

Other models from Biggs (1990), Lyne & Manchester (1988), and Narayan & Vivekanand (1983), henceforth B90, LM88, and NV83 respectively, determine the beaming fraction from the angular beam radius

$$\rho = \rho_0 P^\gamma, \quad (12)$$

where the constants ρ_0 and γ are uniquely defined in each model. Assuming that radio waves are emitted from both poles of the pulsar and that the beams are circular beams, and following TM98 leads to a beaming fraction dependence on magnetic inclination angle of

$$f(\rho, \chi) = \begin{cases} 2 \sin \chi \sin \rho & \chi > \rho, \chi + \rho < \frac{\pi}{2} \\ \cos(\chi - \rho) & \chi > \rho, \chi + \rho > \frac{\pi}{2} \\ 1 - \cos(\chi + \rho) & \chi < \rho, \chi + \rho < \frac{\pi}{2} \\ 1 & \chi < \rho, \chi + \rho > \frac{\pi}{2} \end{cases} \quad (13)$$

Also available is a simple period-independent beaming

model that assumes $f = 0.2$ for all values of P . To determine whether a pulsar is beaming towards us or not, we compare the value of f computed in one of the above ways with a random number between 0 and 1. Only those pulsars for which this random number is less than or equal to f are deemed to be beaming towards us and we move on to the calculations of the final properties of the pulsar.

To describe the location of model pulsars in the Galaxy, we use a regular Cartesian (x, y, z) coordinate system with the Galactic center at the origin and the position of the Sun at $(0, 8.5, 0)$ kpc, again identical to the procedure performed by FK06. Each pulsar’s initial x and y positions on the Galactic plane are determined by randomly choosing a point in the plane of our Galaxy along the spiral arms. We follow the procedure described by FK06 to implement the spiral arm structure. For the radial distribution, we use the form described by Yusifov & Küçük (2004). Then, dispersion away from the plane is used to determine the initial z position. For this, we use an exponential distribution with a mean $z_0 = 50$ pc, and then arbitrarily choose a sign.

To model pulsar birth velocities, we use the optimal model found in FK06, in which the initial velocity components of each pulsar in the x , y and z directions are drawn from exponential distributions with a mean absolute value of 180 km s^{-1} . Although other distributions are available within *evolve*, we do not investigate them any further here. To model the resulting evolution in the Galactic gravitational potential, we follow the method described by Lorimer et al. (1993), where the integration in the gravitational galactic potential is done using a model described by Carlberg & Innanen (1987). From the final position in the model galaxy, we compute the pulsar’s distance from the Sun, d , and its expected dispersion measure (DM) and scatter-broadening timescale at 1 GHz. The latter two quantities are derived using the NE2001 model for the Galactic distribution of free electrons (Cordes & Lazio 2002).

The radio luminosity is calculated, following FK06, with a P and \dot{P} power law dependence, defined by

$$\log L = \log L_0 + \alpha \log P + \beta \log (\dot{P}/10^{-15}) + \delta_L, \quad (14)$$

where L_0 is 0.18 mJy kpc^2 , and δ_L is randomly chosen from a normal distribution with $\sigma_{\delta_L} = 0.8$. The program allows for α and β , two free parameters, to be varied to determine the best functional dependence.

For comparison, we also make available in the code a simple model in which the luminosity is independent of all other parameters. Following FK06, we take the probability, $p(L)$, of a given luminosity as being

$$p(L) \propto \begin{cases} 0 & L \in [0 \text{ mJy kpc}^2, 0.1 \text{ mJy kpc}^2) \\ L^{-\frac{19}{10}} & L \in [0.1 \text{ mJy kpc}^2, 2.0 \text{ mJy kpc}^2) \\ L^{-2} & L \in [2.0 \text{ mJy kpc}^2, \infty). \end{cases} \quad (15)$$

3 MODELING THE OBSERVED PULSAR POPULATION

The steps described above allow us to create a population of synthetic pulsars that are potentially observable. That is, they are deemed to be beaming towards the Earth and the spin-down models we are investigating predict that they are radio-loud. We wish to compare this population with those

pulsars that are potentially detectable by current surveys. Since the primary objective of this work is to reproduce and extend upon the work of FK06, in this paper, we focus on the sample of pulsars detectable by the Parkes Multibeam (see Lorimer et al. 2006, and references therein, hereafter PMB) and Swinburne (Edwards et al. 2001, hereafter SMB) multi-beam pulsar surveys. By accurately modeling the detection thresholds of these surveys as described below, and selecting only those model pulsars that are theoretically detectable, we can form samples of model observed pulsars. When FK06 were carrying out their work, the sample of real pulsars detected in these surveys was 1065. In our analysis, we will use the sample of 1135 pulsars currently catalogued. Our criteria is to select all isolated pulsars not associated with a globular cluster and having both $\dot{P} < 10^{-12}$ and $P > 30$ ms.

To form our model observed samples, the first step is to compute the apparent flux density of each model pulsar, S . Following standard practice Lorimer & Kramer (2005), we neglect geometrical factors in the inverse square law relationship and find S from the pulsar’s distance, d , and radio luminosity, L , as follows

$$S = \frac{L}{d^2}. \quad (16)$$

Note that this flux density is defined (following our definition of L) to be at an observing frequency of 1.4 GHz, the frequency at which the PMB and SMB surveys were carried out. For the purposes of this work, no assumptions about the pulsar spectral index distribution are necessary.

To model the detection threshold of the pulsar surveys, it is also necessary to model the pulse widths. Following FK06, we assume that the intrinsic pulse width, W_{int} , is 5% of the pulse period. The observed pulse width, W_{obs} , and signal-to-noise ratio, S/N, are then calculated using the method described in Lorimer et al. (2006) in their Equations 1–7. Pulse width models from recent papers (see, e.g., Smits et al. 2009) have also been considered and are available for use in the code.

All pulsars which lie inside the sky boundaries covered by the two surveys, have $S/N > 9$, and where $W_{\text{obs}} < P$ are deemed detectable and saved for subsequent analysis, as described below. Our simulation proceeds until 1135 pulsars are detected, to match the combined sample found in the PMB and SMB surveys.

4 METHOD FOR COMPARISON

To compare our trial results quantitatively, we use the Kolmogorov-Smirnoff (KS) test, a non-parametric estimator based on the maximum deviation seen in the cumulative distribution of two sample data sets (see, e.g., Press et al. 1986). For a given distribution, the KS test returns a statistic that is used to determine a probability, Q , that two samples came from the same underlying population. As described below, we make use of this probability to investigate whether model pulsar populations are inconsistent with the observed data.

To investigate the sensitivity of the KS test to changing model parameters, we run a single simulation using the optimal parameters from the FK06 model. We then generate four further Monte Carlo realizations of the same model

Table 1. Here we show how the KS probability for the period distribution behaves when given simulated samples that are exactly the same as, similar to, and completely different than an original sample. See text for details of the simulations.

TRIAL #	Q_P (SAME)	Q_P (SIMILAR)	Q_P (DIFFERENT)
1	0.1299	0.0296	$< 10^{-12}$
2	0.8928	0.0094	$< 10^{-12}$
3	0.7397	0.1098	$< 10^{-12}$
4	0.6958	0.1744	$< 10^{-12}$
AVG	0.6145	0.0808	$< 10^{-12}$

and compare them to the original simulation using the KS probability for the period distribution, Q_P . Next, we make a small modification, changing μ_P from 300 ms to 280 ms, run four more simulations and compute Q_P by comparing with our original simulation. Finally, we make a more significant change to the model, changing μ_P to 250 ms, σ_P to 100 ms, and $\mu_{\log B}$ to 12.00. We run four further simulations using these parameters and record Q_P against the original simulation. From the results of these simulations that are summarized in Table 1, we conclude that individual KS probabilities above 10% suggest that two populations are consistent with another, while probabilities in the range 1–10% imply possible differences between populations. However, the steep decline in the KS probability when two populations differ significantly suggest that it is a powerful metric to weigh one model against another.

In this work, we wish to track the multiple observed parameters relevant to our simulations. Therefore, following Bhattacharya et al. (1992), we define a figure of merit for each simulation

$$\text{FOM} = \log[Q_P \times Q_{\dot{P}} \times Q_l \times Q_b]. \quad (17)$$

Here the subscripts on each KS Q value refer to the distributions of period (P), period derivative (\dot{P}), Galactic longitude (l) and Galactic latitude (b).

5 RESULTS AND DISCUSSION

In this section, we will describe and discuss our results. Our main goal is to compare the power law spin-down model (Eq. 2) with the new spin-down model proposed by CS06 (Eq. 9) under a variety of assumptions. The logical flow of our approach is summarized in Fig. 2.

5.1 Simulation Models

We begin by using the basic model parameters from FK06 and applying them to both spin-down laws which we call models 1A and 1B. In this convention “A” refers to the power-law spin-down model and “B” refers to the CS06 spin-down model. Model 2 attempts to improve the original model by changing the luminosity law and using random inclination angles to better match the observed sample. Subsequent models are motivated to be more physically realistic with the incorporation of: angle-dependent beaming models and a range of braking indices for models 3A and 3B, and inclination angle decay for models 4A and 4B.

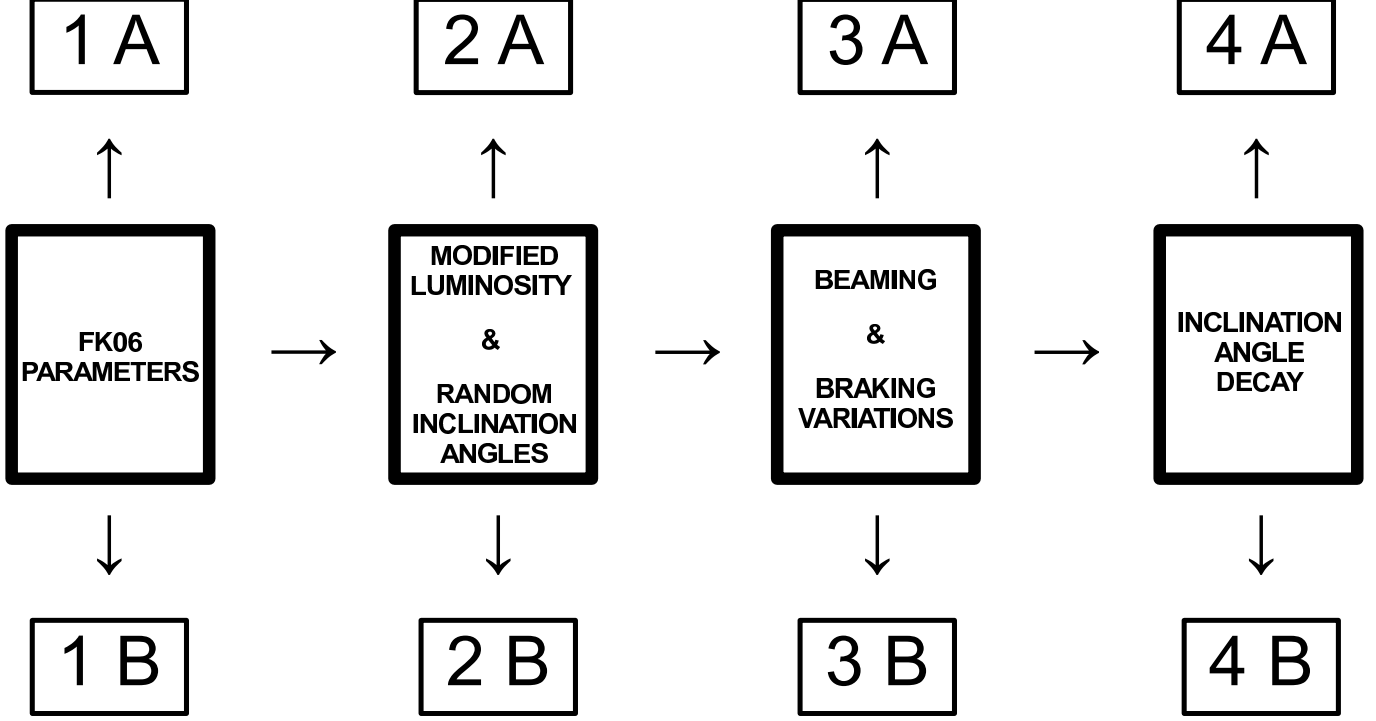


Figure 2. Schematic showing the logical flow of our approach to comparing the power law (A) and CS06 spin-down (B) models. We begin in model 1 by using the best parameters from FK06. As described in the text, subsequent models then contain additional complexity in an attempt to be more physically plausible representations of the true population.

Table 2 provides an overall summary of our results, showing base-10 logarithms of the individual KS probabilities and the FOM for each model. We also compute the mean birth rate (\mathcal{R}) of pulsars required to produce the observed sample sizes for each model. This is defined as the ratio of the *total* number of pulsars generated in each simulation to the maximum age of the population, t_{\max} .

5.1.1 Model 1: FK06 basic parameters

Adopting the optimal parameters found by FK06, we generate model A which is shown in Fig. 3. The histograms show a relatively accurate replication of the original FK06 results. While we are generally able to reproduce the results of FK06, we find somewhat lower KS probabilities for P and \dot{P} than FK06. Obtaining an exact match to results obtained with a different simulation is challenging and the discrepancies we find highlight the difference in the implementation of the model in the two codes. We duplicate most of the major results well. Some other parameters, such as α and β , have to be changed slightly from the values presented in FK06, but we obtain the majority of their results using our code. These changes are addressed in the remaining models.

For model B, we retain all the parameters of model A with the exception of the spin-down law, which we replace by our implementation of CS06 described in Section 2. As evidenced by the results shown in Table 2, the P and \dot{P} distributions are not as well reproduced.

This model has mixed results. Many areas, such as the effect of the alignment angle, the effect of having no angle dependence, and the underlying distribution of pulsars lying below the death line (see Fig. 1, 3, 6 of their paper), can be

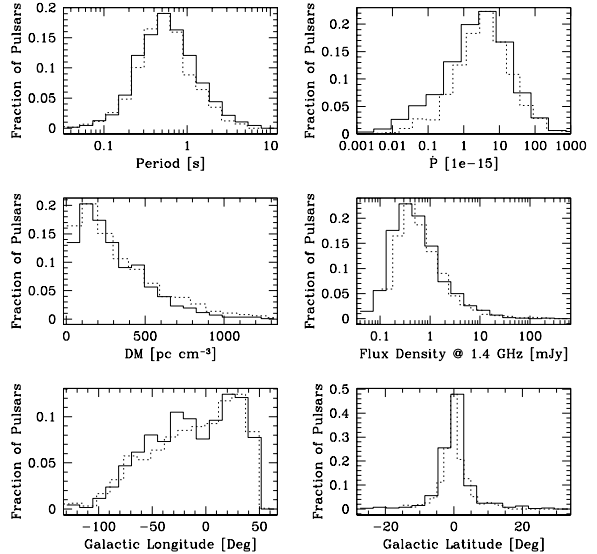


Figure 3. Histograms of some of the key properties from model 1A. The solid histograms represent the observed pulsar population. The dotted histograms are the results of our simulation.

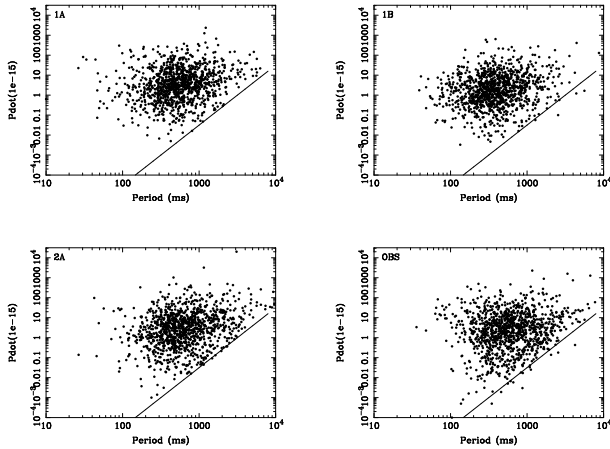


Figure 4. Our resulting $P-\dot{P}$ diagrams, with the adopted death line shown in each plot for reference. Shown in the upper panels are our implementations of FK06 (model 1A, upper left) and CS06 (model 1B, upper right). The lower panels show our improved simulation (model 2A, lower left), which is based on an FK06 spin-down model, and the real observed sample of pulsars (lower right).

replicated with our code. However, the KS statistics are not as high as they are for the FK06 spin-down model. This applies not only to Model 1, but to the rest of the models as well.

5.1.2 Model 2: Modified luminosity law and random inclination angles

In an attempt to improve the low KS statistics seen in the P and \dot{P} distributions for model 1, we search a range of different luminosity indices. Using Equation 14, we vary α from -1.9 to -0.8 and β from 0.1 to 0.9 . Our best result occurs when α and β take the values of -1.0 and 0.5 , while FK06 found optimal values of -1.5 and 0.5 . As discussed in FK06, simulation techniques vary from model to model, and small deviations may occur between models in the search for optimal parameters.

So far we have assumed orthogonal rotators in the spin-down models. A more realistic and self-consistent approach is now followed by assigning random inclination angles to all pulsars.

The results from model 2 are significantly better than model 1, as seen in Table 2. At this point, we can see how much improvement is gained by changing only two parameters, so we move on to test other parameters to see if this improvement continues.

5.1.3 Model 3: Beaming model and braking index variations

Motivated by the improvements seen in model 2, we now relax the requirement for the braking index $n = 3$ and allow a range of braking indices. Based on the observed sample, a sensible choice is to select n from a flat distribution in the range $2.5 < n < 3.0$.

Our previous models adopt the TM98 beaming model, which is used in FK06. However, we now consider computing

the beaming fraction based on a period-dependent opening angle law.

These results are worse than the previous model in terms of KS statistics, however, they are still better than the original model. For model A, the birthrate decreases from nearly 4 pulsars per century to a more acceptable 3 per century. However, model B has just the opposite trend: the birthrate changes from 3 to 4 pulsars per century.

5.1.4 Model 4: Inclination angle decay

Our final model is motivated by the recent results of WJ08, who found evidence for alignment of the spin and magnetic axes. In both models 4A and 4B, the initially random inclination angles decay according to Eq. 1 with an exponential decay timescale of $t_d = 10^7$ yr. Model 4A uses the spin-down law found in Eq. 7 while model 4B assumes the CS06 relation given in Eq. 9. As shown in Table 2, both models perform very poorly, with significantly lower figures of merit than the earlier models without alignment. For the case of model 4A, this poor agreement can be understood when it is seen that Eq. 7 is essentially equivalent to an exponential decay of the magnetic field — more generally, an exponential decay of the braking torque. From the work of FK06, and preliminary simulations we have carried out, we know that a decaying braking torque is inconsistent with the observations. For the case of model 4B, the strong dependence on the spin-down model (Eq. 9) with χ is also the reason for the low figure of merit.

These results present a dilemma. On one hand, the empirical evidence for alignment presented by WJ08 appears to be very robust. On the other hand, we have found that magnetic dipole spin-down laws provide a good description of the population without inclination angle decay. The spin-down laws we have implemented depend critically on this inclination angle. This implies that one way to resolve the discrepancy is to modify the spin-down law so that inclination angles are removed. While there is no physical basis for taking the $\sin^2 \chi$ term out of Eq. 3, we find that a modified version of model 4A which uses Eq. 5 instead of Eq. 7 does produced improved results, though the overall FOM (-6) is still lower than seen for the other models. In a future paper, we intend to investigate this issue further. Based on our current results, however, it appears that the braking torque on a pulsar is independent of its magnetic inclination angle.

Finally, for completeness, we have compared models 2A, 3A, and 4A with the pulse width model mentioned in Smits et al. (2009). The birthrates for all three trials remain consistent with each model, however, the KS statistic FOM is generally worse. We conclude that changing the way in which pulse widths are modeled will not improve our results.

5.2 Individual parameters

Separate from our optimal models, we test various pulsar parameters by themselves in order to gain a better understanding of how they affect the resulting pulsar population. In this section, we take a closer look at each of these parameters.

Table 2. Summary of KS statistics, figures of merit (FOM) and birth rate (\mathcal{R}) comparing FK06 with the four models considered in this paper. See text for details of the various models.

Parameter	FK06	Model 1		Model 2		Model 3		Model 4	
		A	B	A	B	A	B	A	B
P	-2.15	-1.68	-12.0	-0.94	-7.00	-1.75	-12.0	-12.0	-10.7
\dot{P}	-1.20	-4.41	-5.35	-0.51	-0.67	-0.08	-1.76	-6.37	-2.21
l	-0.90	-0.12	-0.12	-0.07	-0.09	-0.28	-0.40	-0.10	-0.25
b	-1.14	-0.50	-0.13	-0.23	-0.30	-0.95	-1.87	-1.01	-1.56
FOM	-5.39	-6.71	-17.6	-1.75	-8.06	-3.06	-16.0	-19.5	-14.7
\mathcal{R} (psrs/century)	2.8	3.85	1.97	3.56	2.84	2.97	3.75	5.31	3.68

5.2.1 Beaming

We run multiple simulations to test the beaming models. For each trial, we alter only which beaming model is to be tested, and leave all other parameters the same. The constant beaming fraction model, or one in which 20% of all pulsars beam towards Earth, and the NV83 beaming model both give poor results. The KS statistics using these models are very close to zero for all simulations.

The beaming models of LM88, B90, and TM98 each give much better results. The TM98 model yields the best population of pulsars, but it is not statistically better than the other two models. Finally, we try a period-dependent model, similar to one described in WJ08. This gives us our best result overall result in terms of KS statistics and birthrates.

Based on these results, we can say a requirement for the population is a period-dependent beaming model, as well as small opening angles, similar to LM88, B90, and TM98. These three beaming models, along with WJ08, are all statistically about the same.

5.2.2 Braking Index

As a test of braking indices, we use our simulation Model 2A. We try indices ranging from 3.2 to 2.5, as well as a very realistic random model in which indices are chosen at random between 2.5 and 3.0. We find very few differences when varying the braking indices, as shown in Table 3. Due to the lack of any significant difference between various braking indices, we can adopt the realistic random model for use in our simulations.

It is useful to again look back at the A models from Table 2. We notice a decrease in birthrate when going from model 2 to model 3. The two parameters that are altered between the two models are the braking index and the beaming model. The results presented in Table 3 make it clear that this drop in birthrate is not entirely due to the braking indices, and thus the angle-dependent beaming model must affect the birth rate as well.

5.2.3 Luminosity

We run many luminosity simulations by changing the power law indices of P and \dot{P} . The best result we obtain yields indices of -1.0 for P and 0.5 for \dot{P} . Our trials also include a simulation involving random luminosities, i.e. no period dependence. The results are less than ideal, and not close to

Table 3. We show our results from 9 simulations with different values of the pulsars' braking indices. This is an implementation of the our Model 2A, changing only the braking index during each simulation. The resulting birth rate, in units of pulsars born per century, and FOM (as described previously) is shown for comparison purposes.

Braking Index	\mathcal{R} (psrs/century)	FOM
$n = 3.2$	3.75	-3.78
$n = 3.1$	3.99	-4.09
$n = 3.0$	3.56	-1.75
$n = 2.9$	3.51	-1.63
$n = 2.8$	3.52	-2.27
$n = 2.7$	3.53	-3.66
$n = 2.6$	3.25	-1.41
$n = 2.5$	3.28	-2.74
$2.5 < n < 3.0$	3.60	-1.38

the results we obtain when using a period-dependent luminosity distribution. Thus, we conclude that there must be some period dependency for the luminosity. Similar conclusions were reached by FK06, however, their optimal value for the P power law index was -1.5 .

For our ideal simulations, our underlying luminosities have a distribution that is very similar to the log-normal distribution found in Fig. 15 of FK06. In this regard, we note that this distribution provides, in our opinion, the best current estimate of the pulsar luminosity function. Unlike previous power-law models (see, e.g., Lorimer et al. 2006), the log-normal does not require a lower luminosity cutoff and is strongly recommended for studies which require some reasonable assumption about the luminosity function.

5.2.4 Covariances

With such a large number of model parameters in our simulations, we are mindful during our study to keep track of any interdependencies that might be expected. The biggest covariances we find involve the luminosity. Changing the braking index along with the luminosity function can be done in such a way that two very similar results can be obtained with two completely different luminosity distributions and braking indices. For example, $n=3.0$ and power indices of -1.5 and 0.5 could yield the same results as $n=2.7$ and indices of -1.2 and 0.8 . A similar relationship is found between the luminosity and the alignment angle. Running a simulation

with all angles equal to 90° might give similar results to another simulation with all angles equal to 45° and having luminosity indices of -1.8 and 0.9 . Most of these covariances are beyond the scope of this paper, simply due to the large matrix of parameters that would be analysed.

5.2.5 Death line

For completeness, we run simulations of both models that do not use a death line. As one might expect, we obtain an overabundance of high period pulsars that have very low luminosities. Our results here just confirm that, within the framework of the models we have developed here, a death line is indeed required when modeling a distribution of pulsars. While it might be possible to construct a model in future which does not require a death line, we are not currently aware of any straightforward means of achieving this.

6 CONCLUSIONS

We have successfully implemented two pulsar spin-down models and accounted for selection effects as far as possible to synthesize populations of observable radio pulsars. From a statistical comparisons of various models, we have gained a better understanding of how their parameters affect the spin-down evolution of pulsars on a $P-\dot{P}$ diagram. Our main conclusions are as follows:

- The magnetic dipole spin-down model from FK06 works best with our simulations. We are able to reproduce the results from their paper and obtain some improved results by modifying some of their parameters. The model of CS06 produces poorer results. Further modifications of this model appear to be required to improve it.
- The braking index, n , does not have a significant impact on our results. Having a braking index of $n=3.0$ works just as well as the rather unphysical scenario of $n > 3.0$. For our optimal simulation, we use the most realistic model, which picks a random braking index between 2.5 and 3.0 for each pulsar.
- The optimal configuration for magnetic inclination angles is a random distribution. Models in which the inclination angle decays on timescales of $\sim 10^7$ yr do not reproduce the observations well. Further modifications to the spin-down laws appear to be required in order to account for the strong empirical evidence for alignment found by WJ08.
- Pulsar luminosities must have a period dependence. We are able to use a power law for the period and period derivative to replicate the $P-\dot{P}$ diagram. By tweaking the exponents in that law, we can alter the resulting distribution of pulsars on our diagram. Even with period dependent luminosity laws and beaming models, a death line is required to explain the dearth of pulsars in the lower right of the $P-\dot{P}$ diagram.

Studying these relationships between the $P-\dot{P}$ diagram and the various pulsar parameters allowed us to become more aware of covariances, eliminate a few parameter models, and overall obtain better insight to the behaviour of pulsars as they evolve across the $P-\dot{P}$ diagram. Future studies will enable us to further narrow down some parameter models and,

in particular, allow us to investigate the issue of magnetic alignment.

ACKNOWLEDGEMENTS

This work was supported by a West Virginia EPSCoR Research Challenge Grant awarded to the West Virginia University Center for Astrophysics.

REFERENCES

- Arzoumanian Z., Chernoff D. F., Cordes J. M., 2002, *ApJ*, 568, 289
- Bhattacharya D., Wijers R. A. M. J., Hartman J. W., Verbunt F., 1992, *A&A*, 254, 198
- Biggs J. D., 1990, *MNRAS*, 245, 514
- Carlberg R. G., Inman K. A., 1987, *AJ*, 94, 666
- Contopoulos I., Spitkovsky A., 2006, *ApJ*, 643, 1139
- Cordes J. M., Lazio T. J. W., 2002, preprint, *astro-ph/0207156*
- Edwards R. T., Bailes M., van Straten W., Britton M. C., 2001, *MNRAS*, 326, 358
- Faucher-Giguère C.-A., Kaspi V. M., 2006, *ApJ*, 643, 332
- Gold T., 1968, *Nature*, 218, 731
- Gonthier P. L., Ouellette M. S., Berrier J., O'Brien S., Harding A. K., 2002, *ApJ*, 565, 482
- Gunn J. E., Ostriker J. P., 1970, *ApJ*, 160, 979
- Hartman J. W., Bhattacharya D., Wijers R., Verbunt F., 1997, *A&A*, 322, 477
- Johnston S., 1994, *MNRAS*, 268, 595
- Lorimer D. R., Bailes M., Dewey R. J., Harrison P. A., 1993, *MNRAS*, 263, 403
- Lorimer D. R., Bailes M., Harrison P. A., 1997, *MNRAS*, 289, 592
- Lorimer D. R., Faulkner A. J., Lyne A. G., Manchester R. N., Kramer M., McLaughlin M. A., Hobbs G., Possenti A., Stairs I. H., Camilo F., Burgay M., D'Amico N., Corongiu A., Crawford F., 2006, *MNRAS*, 372, 777
- Lorimer D. R., Kramer M., 2005, *Handbook of Pulsar Astronomy*. Cambridge University Press
- Lyne A. G., Manchester R. N., 1988, *MNRAS*, 234, 477
- Lyne A. G., Manchester R. N., Taylor J. H., 1985, *MNRAS*, 213, 613
- Narayan R., Ostriker J. P., 1990, *ApJ*, 352, 222
- Narayan R., Vivekanand M., 1983, *A&A*, 122, 45
- Pacini F., 1968, *Nature*, 219, 145
- Press W. H., Flannery B. P., Teukolsky S. A., Vetterling W. T., 1986, *Numerical Recipes: The Art of Scientific Computing*. Cambridge University Press, Cambridge
- Smits R., Lorimer D. R., Kramer M., Manchester R., Stappers B., Jin C. J., Nan R. D., Li D., 2009, *A&A*, 505, 919
- Tauris T. M., Manchester R. N., 1998, *MNRAS*, 298, 625
- Taylor J. H., Manchester R. N., 1977, *ApJ*, 215, 885
- Weltevredre P., Johnston S., 2008, *MNRAS*, 387, 1755
- Young M. D., Manchester R. N., Johnston S., 1999, *Nature*, 400, 848
- Yusifov I., Küçük I., 2004, *A&A*, 422, 545

APPENDIX A: AN OPEN-SOURCE APPROACH TO PULSAR POPULATION SYNTHESIS

Following the initial version described by Lorimer et al. (2006), the source code used in this work is freely available at <http://psrpop.sourceforge.net>. We briefly describe the new features of the pulsar simulation package, **psrpop**, as well as announce the availability of a website, <http://psrpop.phys.wvu.edu>, used to investigate past and future pulsar surveys.

The biggest new feature of the software package is the ability to evolve a pulsar’s spin period in time. Currently, spin-down models from FK06 and CS06 are available for use in the simulations. By having this evolution feature, we can now watch a pulsar’s life cycle, from birth to death, and observe how its period changes with time. The program also has the ability to use various beaming models, luminosity laws, and alignment angle functions. These allow for further studying of the individual pulsars, and a more complete understanding of pulsar populations as a whole.

The **psrpop** website currently has the capability of surveying any of the eight model populations generated for this paper, and future models will also be available for use. The user can “search” these model populations using previous surveys such as the Parkes Multibeam Survey, theoretical surveys such as one using the proposed Square Kilometer Array, or they can create their own survey. One of the main benefits of running a custom survey is the ability to predict yields of future surveys.

After surveying one of the pulsar populations, the website outputs the total number of pulsars detected, a $P-\dot{P}$ diagram, and a few comparison plots. These plots contain histograms of the pulsar properties detected in the survey that overlay histograms of the observed pulsar population. Some possible properties that can be shown in the histogram plots are pulse period, period derivative, dispersion measure, and flux density.